J. Hydrol. Hydromech., 72, 2024, 2, 207–222
https://doi.org/10.2478/johh-2024-0010
© 2024 Jiangyu Wang et al., published by Sciendo. This work is licensed under the Creative Commons Attribution-NonCommercial-NoDerivatives 4.0 International Licence.

sciendo Journal of Hydrology and Hydromechanics Institute of Hydrology SAS

Flow resistance of emergent rigid vegetation in steady flow

Jiangyu Wang [1], Jinxin Liu [1,2], Yining Sun [1], Ji Li [3], Zhixian Cao [1*]

[1] State Key Laboratory of Water Resources Engineering and Management, Wuhan University, Wuhan 430072, China.
[2] Changjiang Survey, Planning, Design and Research, Co., Ltd., Wuhan 430010, China.
[3] Zienkiewicz Centre for Computational Engineering, Faculty of Science and Engineering, Swansea University, Swansea SA1 8EN, UK.
[*] Corresponding author. E-mail: zxcao@whu.edu.cn

Abstract: Enhanced understanding of flow resistance in open channels with emergent vegetation is essential for flood management and river ecosystem restoration. The presence of vegetation can significantly alter bed resistance, leading to a challenge in accurately predicting flow discharge, water levels, sediment transport, and bed deformation. Previous studies on vegetated flows have focused on vegetation resistance, on which the impact of vegetation has been ignored or poorly estimated. This study proposes a new analytical model, built upon the momentum conservation law, to predict flow resistance to vegetated zones in a plain bed without bed forms, explicitly quantifying bed resistance and vegetation resistance in a corollary manner. The proposed model is benchmarked against five typical sets of laboratory experiments. It is demonstrated that the present model using a modified logarithmic velocity distribution performs best, whereas that assuming a uniform velocity profile considerably overestimates the vegetation resistance and neglects the effect of vegetation on bed resistance. The ratio of bed resistance to the total resistance is shown to range between 5% and 40%, and it decreases with increasing vegetation density and decreases with water depth. Therefore, bed resistance cannot be ignored when modelling shallow water flow with sparsely distributed vegetation. It is also revealed that vegetation arrangements significantly affect flow resistance, and therefore a model incorporating the effect of vegetation arrangement performs better. Overall, the present model facilitates a viable and promising tool for quantifying flow resistance in emergent vegetated channels.

Keywords: Emergent rigid vegetation; Friction velocity; Bed resistance; Vegetation resistance; Momentum conservation equation.

INTRODUCTION

Aquatic vegetation, a ubiquitous feature of natural rivers and floodplains, plays a key role in hydrodynamic (Aberle and Järvelä, 2013; Stephan and Gutknecht, 2002), hydrological (Wohl et al., 2005), geomorphological (Alekseevskiy et al., 2008; Gurnell et al., 2012; Osterkamp and Hupp, 2010), and ecological processes within aquatic environments (Järvelä, 2002). On the one hand, the vegetation may considerably increase flow resistance, slowing down the flow and raising the water levels, so increasing the risk of floods. On the other hand, by changing in velocity distribution and turbulent structures in vegetated channels (Li et al., 2015; Nikora et al., 2013; Wang et al., 2022; Yang et al., 2019), vegetation promotes sediment deposition (Wu and He, 2009), reduces bed erosion and increases bank stability (Vargas-Luna et al., 2016). Furthermore, vegetation is known to provide habitats for aquatic and terrestrial wildlife, beautify the environment, and permeate pollutants (Huai et al., 2018; Liu et al., 2008). Therefore, an improved understanding the dynamics of flow resistance in the vegetated area is of great importance for flood management and river ecosystem restoration (Huai et al., 2015).

The mechanism underlying the resistance to vegetated flows is very complicated because it not only depends on flow properties such as the water level, flow discharge, and shape of the river, but it also closely correlates to vegetation characteristics like density, species, tenacity, shape, and height. During the past several decades, a great deal of research has been carried out on three aspects of vegetated open channel flows, namely, flow resistance characteristics, hydrodynamic characteristics, and the effect of vegetation patterns on flow characteristics, through experimental investigations (Bennett et al., 2002; Liu et al., 2008; Noarayanan et al., 2012; Tanino and Nepf, 2008), numerical simulations (Huai et al., 2009b; Lopez and Garcia, 2001; Poggi et al., 2009) and theoretical analyses (Baptist et al., 2007; Cheng, 2011; James, 2021; Jordanova et al., 2006; Michioku et al., 2014). Many experiments have been conducted in the field and in laboratory flumes using different shapes of natural or artificial materials to model aquatic vegetation arranged in different arrays (uniform, staggered, or random) under various flow and sediment conditions (uniform or non-uniform flow, with or without sediment transport), studying the effect of vegetation on flow resistance and hydraulic characteristics (Wang et al., 2014; Zhang et al., 2020). Based on the measurements of hydraulic parameters like upstream and downstream water levels and flow velocities, insight has been provided into the three-dimensional velocity distribution and turbulent flow structure (Kumar and Sharma, 2022; Li et al., 2014; Nezu and Sanjou, 2008). Noting the importance of estimating the hydraulic resistance, only a few studies have directly measured the drag force acting on vegetation (Armanini et al., 2005; Tinoco and Cowen, 2013; Zhao et al., 2014b), with most researchers using velocity and pressure data to infer the flow resistance. Using parameters such as the drag coefficient (C_d) and Manning's roughness coefficient (n) to estimate vegetation resistance and related as a function of vegetation characteristics or flow parameters (Chapman et al., 2015; Kothyari et al., 2009). However, due to the complexity of the vegetation distribution in the channels, empirical formulas for drag coefficients obtained through experiments differ from the real situations, which means that the physical tests do not match actual conditions.

In addition to experimental studies, various mathematical models, including Reynolds-averaged Navier–Stokes models with isotropic turbulence closure, Reynolds stress models of anisotropic turbulence, and large eddy simulations, have been proposed to simulate flows with aquatic vegetation, probing into flow resistance caused by the effect of vegetation on the mean flow, turbulence statistics, instantaneous flow field, and flow structure change (Huai et al., 2015; Stoesser et al., 2010). In order to quantify the effects of vegetation in terms of flow resistance, the models calculate the velocity field over the whole computational area and provide predictions of water and sediment movement, bed deformation, and so on. Although the aforementioned simulations could accurately predict flow resistance, such models are not widely used due to their complexity and excessive computational cost.

Comparatively, analytical solution models are more attractive because of their advantages of easy implementation and high accuracy. Typically, open channel flows are described by shallow water equations, which are mathematically "closed" by various approximations to the friction slope (S_f). In practice, S_f is inferred from empirical friction equations like Manning's equation by assuming the flow is locally steady and uniform. The key parameter to be specified in this "closure" is the absolute roughness, which may be encoded as Manning's roughness coefficient (n), Chezy's resistance factor (C), or the Darcy-Weisbach friction factor (f). Although these friction coefficients can be obtained empirically or even from photographs or drawings (James, 2021), such approaches are unsuitable for vegetated flows as friction coefficients vary significantly with vegetation factors and flow conditions. Therefore, in terms of vegetated flow modelling, it has become a common practice to use analytical models to determine the flow resistance of vegetated zones. The analytical models are often built upon momentum conservation, a force system, or dimensional analysis, with the effects of vegetation resolved by means of empirical or semi-empirical relations that are established by regression analysis of experimental data (Gu et al., 2007; Hui et al., 2010; Kouwen and Fathi-Moghadam, 2000; Tang et al., 2007; Wu et al., 1999; Wu, 2008). The resulting empirical or semi-empirical friction slope coefficients are commonly used in the simulation of vegetated flows for predicting flood evolution characteristics.

In general, flow resistance in a vegetated open channel mainly includes resistance due to bed roughness and additional resistance caused by vegetation (Stone and Shen, 2002). The presence of vegetation significantly affects bed resistance related to the transport of bed material particles and sediments (Jordanova and James, 2003). Compared with vegetation resistance, bed resistance is not negligible for the incipient motion of the sediment (Wang et al., 2014). However, most of the existing analytical solution models have ignored bed resistance. Although some models have empirically considered bed resistance using the Moody diagram (Stone and Shen, 2002), Colebrook and White formula (James et al., 2004; Rowinski and Kubrak, 2002), or Keulegan equation (Millar, 2000), this may not conform to reality. In order to study mixing processes and river sedimentation in vegetated flows, it is necessary to make a clear distinction between bed resistance and vegetation resistance. An analytical model is not available as yet for quantitatively calculating these two resistances.

In the present work, a new analytical model based on the momentum conservation law is proposed to predict flow resistance in an open channel with emergent rigid vegetation. The bed resistance and vegetation resistance are accurately partitioned and quantified according to the friction velocity. Two modified coefficients (α and β) are introduced to modify the flow velocity distribution and vegetation resistance. Predictions of flow resistance made by the proposed analytical model are compared with five sets of experimental data obtained from Tang et al. (2007), James (2021), D'Ippolito et al. (2019), Cheng and Nguyen (2011) and Zhao et al. (2014a). By considering the ratio of bed resistance to total flow resistance, we analyse the effects of vegetation density, water depth, velocity distribution, and vegetation arrangement on flow resistance.

THEORETICAL MODEL AND METHOD

We consider steady, uniform flow in an open channel with emergent rigid vegetation, assumed to act as multiple circular cylinders. The total resistance to vegetated flow mainly arises from bed roughness and vegetation (Stone and Shen, 2002). Figure 1 indicates the primary force components affecting open channel flow in the presence of emergent rigid vegetation.

Momentum conservation equations

Consider a control volume of the unit bed area stretching from the bed to the water surface. The momentum conservation equation in the streamwise direction is given by

$$\tau_{\text{total}} = \tau_{\text{bed}} + \tau_{\text{veg}} \tag{1}$$

where τ_{total}, τ_{bed} and τ_{veg} are total resistance, bed resistance, and vegetation resistance components.

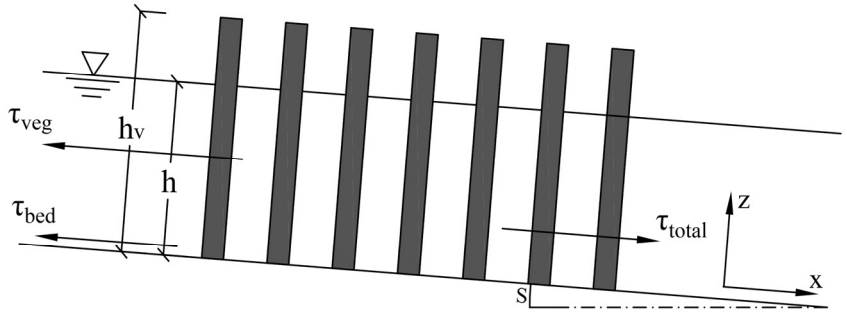

Fig. 1. Force diagram for steady, open channel flow with emergent vegetation. τ_{total} is the component of water weight in the direction of flow, τ_{bed} is the resistance due to bed roughness, τ_{veg} is the resistance caused by vegetation, h is water depth, h_v is the height of vegetation, and S is channel slope.

With the mechanical balance of uniform flow in a vegetated channel, total resistance per unit bed area τ_{total} is balanced by the streamwise gravity component for the control volume of water excluding the volume of vegetation. The mechanical balance equation can be expressed as (Stone and Shen, 2002)

$$\tau_{\text{total}} = \rho g h S(1-\phi) \tag{2}$$

where ρ is the water density, g is gravitational acceleration, ϕ is the vegetation density, defined as $\phi = N\pi D^2/4$, in which N is the number of stems per unit bed area, and D is the cylinder diameter.

The bed resistance τ_{bed} is expressed as

$$\tau_{\text{bed}} = \rho u_*^2 (1-\phi) \tag{3}$$

where u_* is the friction velocity.

When the rigid vegetation is distributed sparsely, the resistance caused by the vegetation per unit of bed area τ_{veg} is a linear superposition of individual forces; that is,

$$\tau_{\text{veg}} = N\int_0^h \mathrm{d}F_{\text{d}} \tag{4}$$

If the resistance of emergent rigid vegetation to the flow is regarded as cylindrical winding resistance, the resistance of a single plant F_{d} per unit length of cylinder at water depth can be expressed as

$$\mathrm{d}F_{\text{d}} = \frac{1}{2} C_d \rho \overline{u}_{(z)}^2 D \,\mathrm{d}z \tag{5}$$

where C_d is the drag coefficient, $u_{(z)}$ is the velocity at water depth z.

The drag coefficient is determined by the relationship between C_d and characteristic Reynolds number $\mathrm{Re_v}$ proposed by Schlichting and Gersten (1979)

$$C_D = \begin{cases} 3.07\,\mathrm{Re_v}^{-0.168}, & \mathrm{Re_v} < 800 \\ 1.0, & 800 \le \mathrm{Re_v} < 8000 \\ 1.2, & 8000 \le \mathrm{Re_v} < 10^5 \end{cases} \tag{6}$$

where the Reynolds number is defined as $\mathrm{Re_v} = u_{(z)} D\cos\theta/\nu$ (–), in which θ is the angle between the vegetation and the vertical direction after bending, for rigid vegetation with no deflection, $\theta = 0$, and ν is the kinematic viscosity of fluid.

Applying momentum conservation in the streamwise direction, the governing equation is given as

$$ghS(1-\phi) = u_*^2(1-\phi) + \frac{1}{2} ND\int_0^h C_d \overline{u}_{(z)}^2 \,\mathrm{d}z \tag{7}$$

Velocity distribution

The presence of emerged vegetation changes the velocity distribution in open channels. Numerous theoretical and empirical formulas have been proposed to approximate the vertical distribution of velocity in a vegetated channel (Gu et al., 2007; Huai et al., 2009a; Klopstra et al., 1997; Zhao and Fan, 2019).

By assuming the streamwise velocity component is uniform with depth, the vegetation resistance can be calculated based on depth-averaged flow velocity (Fathi-Maghadam and Kouwen, 1997; James et al., 2004; Kothyari et al., 2009; Wu et al., 1999; Zhao et al., 2014b). In addition, the logarithmic law and its variants also have been used to describe the vertical velocity profile, evaluate the hydrodynamic roughness height, and quantify the resistance of the emergent vegetation (Afzalimehr and Dey, 2009; Ben Meftah and Mossa, 2016). Here, the vertical velocity distribution is assumed to follow the logarithmic and uniform profiles respectively, and the effect of velocity distribution is analysed by comparing results obtained for different velocity profiles.

(1) Logarithmic velocity profile

Taking into account the effect of emergent rigid vegetation, the velocity distribution is different from the standard logarithmic law, and so a modified coefficient α for the flow distribution is introduced.

$$\frac{u_{(z)}}{\alpha u_*} = \frac{1}{\kappa}\ln\frac{z}{k_s} + B(u_*, k_s) \tag{8}$$

where the modified coefficient of flow velocity distribution α is a function of vegetation density ϕ (α=1 indicates that open channel has no vegetation and there is no modification to the flow resistance), κ is von Karman's constant which is taken as 0.4, k_s is bed roughness height, and $B(u_*, k_s)$ is an integration constant related to the friction velocity and roughness height. Substituting Equation (8) into Equation (4) yields the following expression for vegetation resistance per unit bed area

$$\tau_{\text{veg}} = \frac{1}{2} N\rho D\int_{k_s}^h C_d u_{(z)}^2 \,\mathrm{d}z \tag{9}$$

(2) Uniform velocity profile

If a uniform distribution of velocity is assumed, integrating Equation (4) gives

$$\tau_{\text{veg}} = \frac{1}{2}\beta_0 N\rho Dh\overline{C_d}U^2 \tag{10}$$

where $\overline{C_d}$ is the depth-averaged drag coefficient, taken as 1.0, U is depth-averaged flow velocity, β_0 is a modified coefficient correcting the drag coefficient $\overline{C_d}$ for different vegetation densities. Several studies have revealed that the drag coefficient is greatly affected by many factors related to vegetation especially vegetation density (Kothyari et al., 2009; Liu et al., 2020; Tanino and Nepf, 2008).

Moreover, the depth-averaged flow velocity U can be calculated as below

$$\frac{U}{u_*} = C_z = C_{\text{f}}^{-1/2} \tag{11}$$

where C_z is dimensionless Chézy resistance coefficient, C_{f} is the dimensionless coefficient of the channel bed resistance coefficient.

Substituting Equation (11) into Equation (10), a modified coefficient is explicitly required to modify the vegetation resistance, defined as $\beta = \beta_0 / C_f$. Equation (12) indicates the relationship between friction velocity and vegetation resistance.

$$\tau_{veg} = \frac{1}{2}\beta N \rho D h \overline{C_d} u_*^2 \tag{12}$$

Strategy for resistance calculation

Next, the flow resistance is calculated using the momentum conservation equation (Equation (7)) and the expressions for vegetation resistance (Equation (9) or (12)).

Step 1: Solving for the friction velocity u_*.

If the vertical velocity distribution follows logarithmic profile and the vegetation resistance can be modelled by Equation (9), the friction velocity is solved by applying the bisection method to the momentum conservation equation (i.e., Equation (7)) with the upper and lower limits of initial iteration set as 0.001 m/s and 1 m/s. When the relative error is less than 10^{-6}, the iteration terminates. If the flow velocity is assumed to be uniform in vertical, the friction velocity can be directly obtained by integrating Equations (7) and (12).

Step 2: Solving for bed resistance $\tau_{bed,cal}$ and vegetation resistance $\tau_{veg,cal}$.

Based on the friction velocity obtained in Step 1, the bed resistance and vegetation resistance can be calculated by using Equations (3) and (4) respectively. It should be noted that the modified coefficients for the flow velocity distribution and the vegetation resistance need to be specified in advance, the values determined from experimental data.

DATA COLLECTION AND PRE-PROCESSING

Since the bed resistance and vegetation resistance are difficult to be directly measured in experiments, this paper applies the continuity equation and flow properties such as flow discharge, water depth, and bed slope to approximate the friction velocity and then the resistances. The relative error with respect to the experimental momentum equation is used to determine the modified coefficient of velocity distribution α, after which the modified coefficient of vegetation resistance β can be quantified based on the experimental resistance after modifying the logarithmic velocity distribution.

Laboratory experiments

Five sets of experimental data are collected from previous studies to test and verify the proposed model. All the experimental runs are conducted under steady, uniform flow conditions with the vegetation configured in a linear array (D'Ippolito et al. 2019; Tang et al., 2007) or staggered pattern (Cheng and Nguyen, 2011; James, 2021; Zhao et al.,2014a).

Tang et al. (2007) conducted their experiments in a glass-sided, rectangular circulation flume with vegetation modelled using fixed aluminium cylinders of diameter 0.006 m. James (2021) utilised 0.11 m diameter fixed circular cylinders to represent different vegetation densities on a smooth vinyl bed and a rough bed composed of a single layer of crushed gravel. D'Ippolito et al. (2019) conducted experiments on two sets of small wooden, circular cylindrical rods (of diameters 0.008 and 0.01 m) located near the centre of a variable-slope hydraulic flume with PVC bottom and plexiglass walls. The drag force was directly measured by a calibrated load cell with sensitivity of around 0.001N. The experiments of Cheng and Nguyen (2011) were carried out in a tilting, rectangular flume, with glass side walls and a steel bottom. The middle area of the flume contained a zone, 9.6 m long and 0.3 m wide, in which the vegetation was simulated using arrays of rigid, cylindrical rods of diameter 0.0032, 0.0066, and 0.0083 m. Zhao et al. (2014a) conducted experiments in a laboratory flume with Rigid Perspex cylinders (8.3 mm in diameter), spacing 0.06 m in a staggered pattern. Table 1 provides a summary of the different experimental datasets considered herein, and Figure 2 illustrates the configuration of the vegetation arrays. In this paper, only the experiments with fixed bed are considered.

The first experimental group contains data from Tang et al. (2007) and James (2021) and is used to determine the modified coefficients α and β. The other three sets of experimental data attributed to the second group are used to validate the results obtained from the first group. It is noted that only those cases with vegetation density ranging between 0 and 3% are selected for validation.

Estimation of experimental resistance

(1) Determination of bed roughness height without vegetation.

The logarithmic velocity profile Equation (8) is described by the modified coefficient $\alpha = 1$ and friction velocity $u_* = \sqrt{gRS}$ in non-vegetated cases. The bed roughness height is obtained by fitting to the depth-averaged flow velocity.

$$Q = B\int_0^h u_{(z)}\,\mathrm{d}z \tag{13}$$

where Q is flow discharge, R is hydraulic radius.

(2) Estimation of experimental bed resistance $\tau_{bed,exp}$ and vegetation resistance $\tau_{veg,exp}$.

Given that values of the velocity distribution modified coefficient α, vegetation characteristic parameters, and flow properties such as flow discharge Q, water depth h, and channel slope S are already specified, the experimental bed resistance and vegetation resistance are calculated from

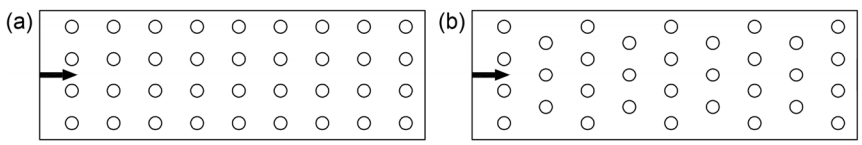

Fig. 2. Configurations of the vegetation arrays (top view): (a) linear; (b) staggered.

Table 1. Summary of experimental data used in the five sets of experiments.

Investigators	Flume width B (m)	Vegetation parameters ϕ (–)	Vegetation arrangement	Note
Tang et al. (2007)	0.420	0.0283	linear	Used for parameter calibration
		0.0113		
James (2021)	2.000	0.0151	staggered	
		0.0303		
D'Ippolito et al. (2019)	0.382	0.0078	linear	Used to test calibrated model
		0.0097		
		0.0297		
Cheng and Nguyen (2011)	0.300	0.0043	staggered	
		0.0192		
		0.0298		
Zhao et al. (2014a)	0.300	0.0130	staggered	

Equations (3) and (4) after estimating the friction velocity from the continuity equation (Equation (13)). When $\alpha = 1$, the results represent experimental resistance without the velocity distribution modification.

Theoretically, Equation (7) strictly follows the momentum conservation law. However, due to measurement error, the two sides of the equation may not strictly balance. To quantify this discrepancy, the relative error for the experimental momentum equation is defined as

$$ERR = \frac{\left|\tau_{\text{bed}} + \tau_{\text{veg}} - \tau_{\text{total}}\right|}{\tau_{\text{total}}} \times 100\% \tag{14}$$

Moreover, relative errors in bed resistance and vegetation resistance are introduced to describe quantitatively the discrepancy between the experimental and calculated results, as follows

$$ERR_{\text{bed}} = \frac{\left|\tau_{\text{bed,cal}} - \tau_{\text{bed,exp}}\right|}{\tau_{\text{bed,exp}}} \times 100\% \tag{15}$$

$$ERR_{\text{veg}} = \frac{\left|\tau_{\text{veg,cal}} - \tau_{\text{veg,exp}}\right|}{\tau_{\text{veg,exp}}} \times 100\% \tag{16}$$

Determination of modified coefficient for flow velocity distribution α

In general, vegetation density is the main factor affecting the modified coefficient for velocity distribution. The relationship between the coefficient and the vegetation density is determined from the experimental data. Note that the modified coefficient is taken as 1 without the presence of vegetation $\phi = 0$. The steps are as follows:

Step 1: Determination of flow velocity distribution modified coefficient for single vegetation density.

Given an arbitrary modified coefficient α, the relative error of the experimental momentum equation ERR_i is calculated for all cases with the same vegetation density. The root mean square error (RMSE) of the experimental momentum equation is used to reflect the error in cases involving a single value of vegetation density.

$$\text{RMSE}_{\text{total}} = \sqrt{\frac{1}{n}\sum_{i=1}^{n} ERR_i^2} \tag{17}$$

The factor n in Equation (17) is the number of cases corresponding to a single value of vegetation density. The value of α corresponding to the smallest RMSE is the flow velocity distribution modified coefficient for a single vegetation density.

Step 2: Fitting an expression for the modified coefficient with respect to vegetation density.

Based on the results from Step 1, the relationship of the modified coefficient α with vegetation density ϕ was fitted by a quadratic equation.

Determination of modified coefficient for vegetation resistance β

Like the flow velocity distribution modified coefficient α, the modified coefficient for vegetation resistance β is primarily influenced by vegetation density herein. The corresponding relationship between β and vegetation density is determined from the relative errors in bed resistance and vegetation resistance. The modified coefficient β is calculated based on the results of α. The procedure involves the following steps:

Step 1: Determination of vegetation resistance modified coefficient for single vegetation density.

For each set of cases with the same vegetation density, the sum of the relative errors in bed and vegetation resistance (ERR_{bed} and ERR_{veg}) is calculated for an arbitrary value of the modified coefficient β. The RMSE of resistance is used to represent the overall error for all cases at this vegetation density, and the modification to the drag coefficient for a single vegetation density is equal to the value of β corresponding to the smallest RMSE.

$$\text{RMSE}_{\text{force}} = \sqrt{\frac{1}{n}\sum_{i=1}^{n}\left(ERR_{\text{bed}} + ERR_{\text{veg}}\right)_i^2} \tag{18}$$

where $\left(ERR_{\text{bed}} + ERR_{\text{veg}}\right)_i$ is the sum of the relative errors in bed resistance and vegetation resistance for the i-th case, and the experimental resistance with such relative error is taken as the corresponding value when modified the logarithmic velocity distribution.

Step 2: Fitting an expression for the modified coefficient with respect to vegetation density.

Based on the results from Step 1, the relationship between the modified coefficient β and vegetation density ϕ was fitted by a linear equation.

RESULTS AND DISCUSSION

Calibration results

Based on the experimental data of Tang et al. (2007) and James (2021), the modified coefficients for flow velocity distribution α and vegetation resistance β were determined using $RMSE_{total}$ and $RMSE_{force}$ respectively. Table 2 shows the values of two modified coefficients (α and β) corresponding to vegetation density ϕ for the first experimental group. The logarithmic velocity distribution also satisfies the condition that $\alpha = 1$ when $\phi = 0$. Therefore, the relationship between the modified coefficient α and vegetation density is fitted with a quadratic function, while β is fitted with a linear function. Accordingly, the following relationships are obtained,

$$\alpha = -316\phi^2 - 5.78\phi + 1 \tag{19}$$

$$\beta = -9333\phi + 403.5 \tag{20}$$

Table 3 provides the RMSE of the experimental momentum conservation equation and flow resistance for calibration cases.

The RMSE for unmodified logarithmic velocity profile is obviously larger than the errors for the other two velocity distributions, indicating that the velocity distribution of open channels with emergent rigid vegetation is no longer conforms to the original logarithmic velocity distribution. The error analysis shows that after modifying the logarithmic velocity distribution of the present model, the maximum relative error of the experimental momentum equation is only 11.44% and the average root mean square error is smaller than 6.00%; after modifying the vegetation resistance of the present model, the average root mean square error of the resistance is less than 6.45%.

As illustrated in Figure 3, the results with modification of the velocity distribution are significantly improved at high vegetation density. When the vegetation is densely arranged, the resistance to vegetated flow increases, reducing the flow velocity and thus leading to a relatively uniform distribution, therefore the modified coefficients α and β in Equations (19) and (20) are negatively related to the vegetation density. Therefore, the proposed analytical solution model is viable for estimating the resistance of emergent rigid vegetated flows.

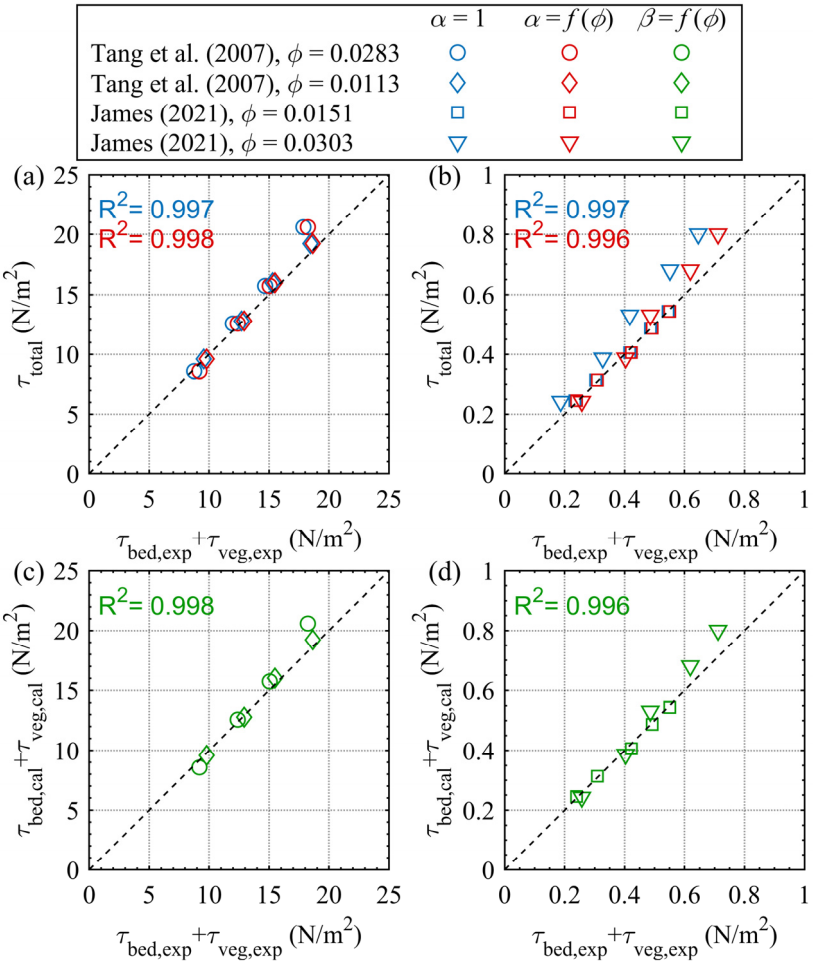

Fig. 3. Calibration results of the present model for the first experimental group: (a–b) comparison of the total resistance τ_{total} *vs.* experimental flow resistance $\tau_{bed,exp} + \tau_{veg,exp}$ using unmodified and modified logarithmic velocity profiles; (c–d) comparison of experimental and calculated flow resistance ($\tau_{bed,exp} + \tau_{veg,exp}$ *vs.* $\tau_{bed,cal} + \tau_{veg,cal}$) using vegetation resistance modification under uniform velocity distribution.

Table 2. Modified coefficients for velocity distribution α and vegetation resistance β corresponding to vegetation density ϕ.

Experiments	ϕ (–)	α (–)	β (–)
Tang et al. (2007)	0.0283	0.49	70
	0.0113	0.78	168
James (2021)	0.0151	0.97	379
	0.0303	0.61	183

Table 3. The RMSE of experimental momentum equation and resistance for calibration cases.

Experiments	ϕ	$\alpha=1$ RMSE$_{total}$ [a]	$\alpha=f(\phi)$ RMSE$_{total}$ [b]	$\beta=f(\phi)$ RMSE$_{force}$ [b]
Tang et al. (2007)	0.0283	7.869	7.122	7.648
	0.0113	2.988	2.402	2.454
	Average [c]	5.952	5.315	5.679
James (2021)	0.0151	2.753	2.324	2.277
	0.0303	19.825	8.164	8.853
	Average	14.153	5.989	6.452

[a] α=1, RMSE$_{total}$ represents the root mean square error (RMSE) of the experimental momentum equation using the unmodified logarithmic velocity profiles.

[b] $\alpha=f(\phi)$, RMSE$_{total}$ and $\beta=f(\phi)$, RMSE$_{force}$ represent the RMSE of the experimental momentum equation using modified logarithmic velocity profiles of the present calibrated model and the RMSE of resistance using modified uniform velocity distribution of the present calibrated model, respectively.

[c] Average is a weighted average of the relative errors at different vegetation densities.

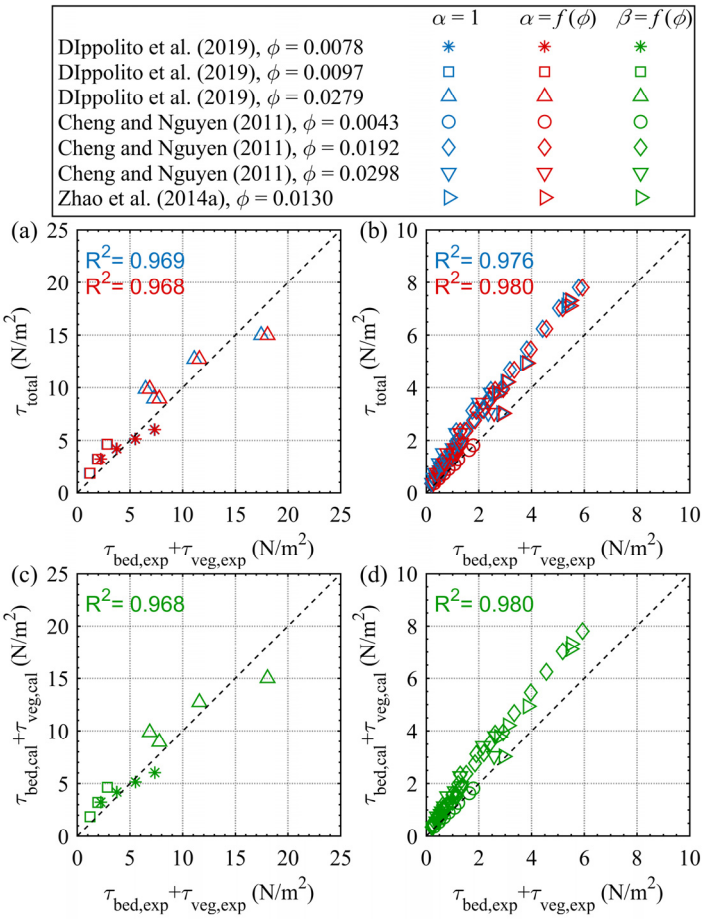

Fig. 4. Validation results of the present calibrated model for the second experimental group: (a-b) comparison of the total resistance τ_{total} *vs.* experimental flow resistance $\tau_{bed,exp}+\tau_{veg,exp}$ using unmodified and modified logarithmic velocity profiles; (c-d) comparison of experimental and calculated flow resistance ($\tau_{bed,exp}+\tau_{veg,exp}$ *vs.* $\tau_{bed,cal}+\tau_{veg,cal}$) using vegetation resistance modification under uniform velocity distribution.

Validation results

Next, the experimental data from D'Ippolito et al. (2019), Cheng and Nguyen (2011) and Zhao et al. (2014a) are revisited to validate the present calibrated model using the two modified coefficients α and β. Figure 4 shows the validation results for the second experimental group, and Table 4 presents the RMSE of the experimental momentum conservation equation and flow resistance, calculated using the present calibrated model. Noted that $\alpha = f(\phi)$ and $\beta = f(\phi)$ are the modifications in velocity distribution and vegetation resistance of the present model.

The predictions by the present calibrated model are in overall good agreement with the measured data, but the validation errors are slightly larger than those in calibration, which may be related to the values of two modified coefficients. Vegetation and flow conditions could significantly affect the resistance calculation. This paper used two sets of cases for calibration, including two sets of vegetation arrangements and vegetation densities, and fitted the approximate relationship between two modified coefficients and the vegetation densities. If more cases with different vegetation densities can be considered to calibrate the modified coefficients, more accurate functional relationships between the modified coefficients and vegetation densities can be obtained, and the validation results will be improved. For D'Ippolito et al. (2019), the reason for substantial computational errors, except for the aforementioned relation to the value of the correction coefficients, may also be the presence of hydraulic jump at the upstream and downstream of the vegetation zone mentioned in the text, resulting in the discrepancy in two sides of the momentum equation. Overall, the foregoing results further demonstrate the capability of the proposed analytical model in predicting the resistance of channels containing emergent vegetation and confirm the need to include its effect in numerical models.

Effect of velocity distribution

Resistance to vegetated flow is affected by many factors such as water flow conditions. The vertical velocity distribution is important because it relates directly to flow capacity and channel resistance. For this reason, this section aims to examine the effect of velocity distribution on resistance to vegetated flow by comparing experimental dimensionless resistance with predictions for different velocity profiles.

Figure 5 compares the calculated splitting ratios of bed resistance and vegetation resistance to total resistance with the experimental values, and Table 5 lists the root mean square errors of predicted resistance ratio and flow discharge using the present calibrated model for different flow velocity distributions. The model with the modified logarithmic velocity distribution performs better than models using an unmodified logarithmic velocity profile or assuming uniform velocity distribution. Furthermore, although the model assuming uniform velocity distribution is simple to use in engineering practice, it obviously overestimates vegetation resistance and ignores the influence of vegetation on bed resistance. In addition, since an accurate resistance coefficient in the presence of emergent rigid vegetation is not available, the model using uniform velocity profile cannot estimate the flow discharge. In contrast, the flow discharge for vegetation densities in the range of 0-3% can be reasonably resolved by the models assuming a modified logarithmic velocity distribution with RMSE of approximately 12%. Briefly, the model using a modified logarithmic velocity distribution leads to the best resistance calculations and also accurately estimates flow discharges especially when the vegetation is dense.

Resistance division

It remains poorly understood whether or not the bed resistance can be ignored in vegetated flow modelling. In order to provide a theoretical basis for sediment transport and river restoration, better knowledge is required of the resistance variation law for vegetated flows. Thus focusing on the relationship between the splitting resistance ratios with vegetation density and water depth in this section.

Based on predictions by the present calibrated model assuming the modified logarithmic velocity profile, Figure 6 shows the splitting ratios of bed resistance and vegetation resistance to total resistance against vegetation density and water depth. As can be seen from Figure 6, the splitting ratio of bed resistance varies between 5% and 40%, whereas that of vegetation resistance is always greater than 60%. Moreover, with the increase of vegetation density and water depth, the splitting ratio of bed resistance decreases and that of vegetation resistance increases, implying the increasing importance of vegetation in deep water with heavily distributed vegetation. Comparatively, if the vegetation is sparsely distributed in a relatively shallow water flow, the bed resistance becomes more important and cannot be ignored, especially when sediment transport is involved.

Table 4. The RMSE of experimental momentum equation and resistance for validation cases.

Experiments data of	ϕ	$\alpha = 1$	$\alpha = f(\phi)$	$\beta = f(\phi)$
		$RMSE_{total}$	$RMSE_{total}$	$RMSE_{force}$
D'Ippolito et al. (2019)	0.0078	20.393	20.107	24.987
	0.0097	39.492	37.701	60.775
	0.0279	22.137	19.910	25.026
	Average	27.473	26.054	38.238
Cheng and Nguyen (2011)	0.0043	9.448	8.078	9.282
	0.0192	39.554	35.265	57.554
	0.0298	43.214	34.972	57.557
	Average	38.127	32.874	53.688
Zhao et al. (2014a)	0.0130	24.580	23.081	30.073

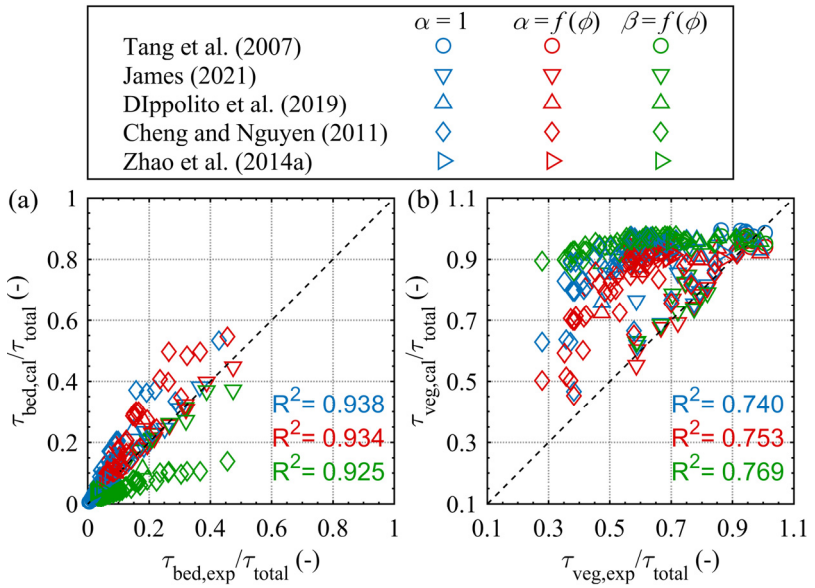

Fig. 5. Comparison of the calculated splitting resistance ratios versus experimental values under different flow velocity distributions for five sets of experiments: (a) comparison of calculated versus experimental values of bed resistance ratio ($\tau_{bed,exp}/\tau_{total}$ *vs.* $\tau_{bed,cal}/\tau_{total}$); (b) comparison of calculated versus experimental values of vegetation resistance ratio ($\tau_{veg,exp}/\tau_{total}$ *vs.* $\tau_{veg,cal}/\tau_{total}$).

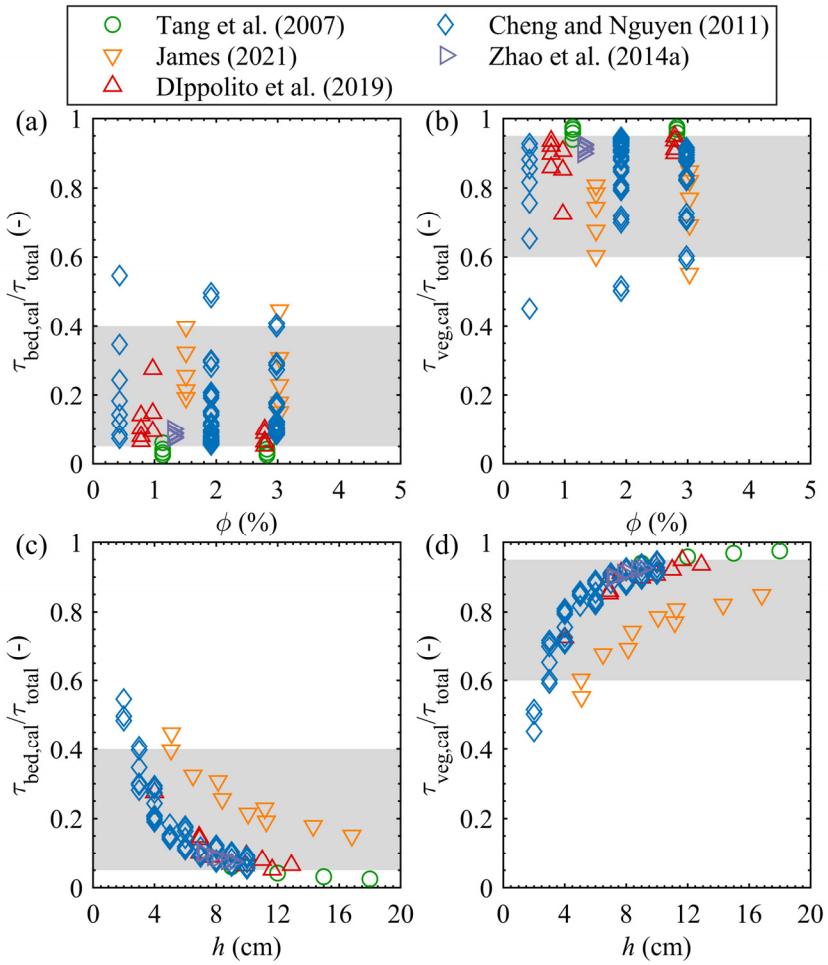

Fig. 6. Variation of resistance ratio predicted using the calibrated models with vegetation density and water depth.

Table 5. The RMSE of splitting resistance ratios and flow discharge using the present model under different flow velocity distributions.

Parameters	Experiments data of	RMSE (%)		
		$\alpha = 1$	$\alpha = f(\phi)$	$\beta = f(\phi)$
τ_{bed}/τ_{total}	Tang et al. (2007)	6.95	5.923	12.504
	James (2021)	16.741	6.382	10.181
	D'Ippolito et al. (2019)	42.871	38.765	43.023
	Cheng and Nguyen (2011)	78.413	58.27	52.103
	Zhao et al. (2014a)	34.513	31.470	34.986
	Average	64.845	48.870	45.059
τ_{veg}/τ_{total}	Tang et al. (2007)	6.640	5.671	5.514
	James (2021)	17.880	6.489	7.431
	D'Ippolito et al. (2019)	41.706	38.151	49.060
	Cheng and Nguyen (2011)	69.672	52.721	85.980
	Zhao et al. (2014a)	33.567	30.922	29.883
	Average	58.101	44.627	70.799
Q	Tang et al. (2007)	2.789	4.214	/
	James (2021)	7.612	3.825	/
	D'Ippolito et al. (2019)	12.725	11.621	/
	Cheng and Nguyen (2011)	14.340	14.268	/
	Zhao et al. (2014a)	9.076	8.193	/
	Average	12.672	12.308	/

Effect of vegetation arrangement on resistance

Except for water flow conditions, the effect of vegetation arrangement on flow resistance has not yet been clarified. In general, for the same flow discharge and vegetation density, a staggered arrangement of vegetation produces larger resistance than for the linear configuration, resulting in higher water levels, smaller flow velocities, and lower conveyance capacity. This is confirmed by comparing the results of D'Ippolito et al. (2019) and Cheng and Nguyen (2011), as shown in Figure 4. D'Ippolito et al.'s (2019) experiments are characterized by a linear array, and so the data are almost scattered about the 45° line. By comparison, the data due to Cheng and Nguyen's (2011) experiments are all above the 45° line. Therefore, the following modified coefficient, which considers the effect of vegetation arrangement, γ, is introduced into vegetation resistance Equation (9),

$$\tau_{veg} = \frac{1}{2}\gamma N \rho D \int_{k_s}^{h} C_d u_{(z)}^2 \, \mathrm{d}z \tag{21}$$

The modified coefficient for the vegetation arrangement in the above equation is determined from experiments in advance, following a similar procedure to that used for determining α. For each group with the same vegetation density, the value of γ corresponding to the minimum RMSE of the experimental momentum equation is evaluated. The condition that $\gamma = 1$ when the vegetation is arranged linearly is also satisfied. According to the above results, the model using the modified logarithmic velocity distribution performs the best, and therefore the modified coefficient α is determined by Equation (19).

In this section, data from Cheng and Nguyen (2011) are used to calibrate and validate the modified coefficient γ. The relative error of the experimental momentum equation is compared for each case with the same vegetation density, and cases corresponding to the maximum and minimum absolute value are selected for calibration, while the rest of the cases are used for validation. Due to the large number of cases with the vegetation density of 1.92%, two more cases are also considered when determining γ. Table 6 gives the values of modified coefficient for vegetation arrangement γ corresponding to vegetation density ϕ.

Figure 7 compares the measured and predicted flow resistance and discharge calculated using the present calibrated model with and without the vegetation arrangement modification. Table 7 details the RMSE for each variable at different vegetation densities. Although the error in calculating the flow discharge increases slightly, the model performance in predicting flow resistance has been improved after introducing the modified coefficient for vegetation arrangement. Specifically, the average RMSE of the experimental momentum equation, bed resistance ratio, and vegetation resistance ratio are reduced by 20.1%, 39.7% and 36.1% respectively.

It is demonstrated that the vegetation arrangement modified coefficient γ does not vary positively with vegetation density ϕ, but instead increases with the number of vegetation plants per unit bed area N. This explains why there is a large discrepancy between the results obtained using the experimental momentum equation for the cases studied by Cheng and Nguyen (2011) and James (2021). Although both experiments were conducted in open channels with staggered vegetation, James (2021) used circular cylinders of larger diameter, resulting in a significantly smaller number of vegetation elements per unit bed area. Therefore, the effect of vegetation on water flow is not as evident as in Cheng and Nguyen (2011), and the relative errors in resistance calculation are smaller.

Table 6. Modified coefficient for vegetation arrangement γ corresponding to vegetation density ϕ.

Experiments data of	ϕ (–)	γ (–)
Cheng and Nguyen (2011)	0.0043	1.06
	0.0192	1.55
	0.0298	1.42

Table 7. The RMSE of flow resistance using the present calibrated model of both unmodified and modified vegetation arrangement at different vegetation densities.

ϕ (–)		RMSE (%)			
		ERR	τ_{bed}/τ_{total}	τ_{veg}/τ_{total}	Q
0.0043	$\gamma=1$	6.577	7.736	7.065	18.951
	$\gamma=f(\phi)$	4.237	4.761	4.352	20.825
0.0192	$\gamma=1$	34.858	60.163	54.838	13.956
	$\gamma=f(\phi)$	12.131	15.979	14.609	23.031
0.0298	$\gamma=1$	34.904	60.835	55.327	10.371
	$\gamma=f(\phi)$	16.020	21.997	20.036	15.998
Average	$\gamma=1$	32.875	56.853	51.783	13.732
	$\gamma=f(\phi)$	12.800	17.159	15.660	20.978

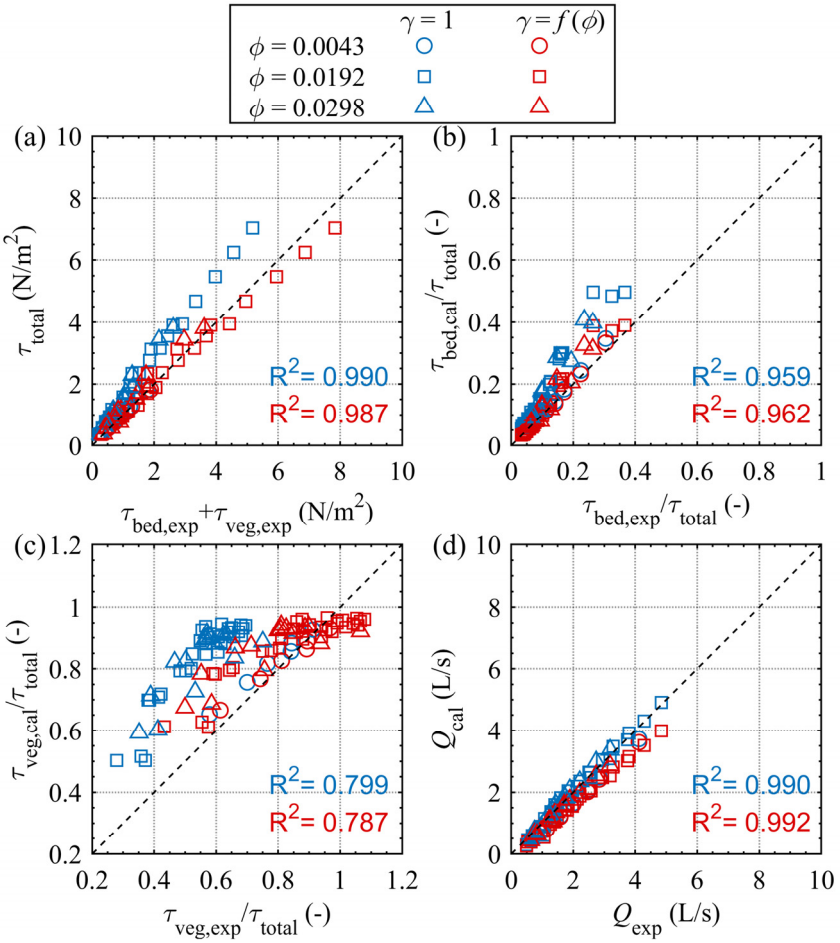

Fig. 7. Comparisons of experimental and calculated flow resistance for the present calibrated model with unmodified and modified vegetation arrangement. (a) Momentum conservation equation (total resistance τ_{total} *vs.* experimental flow resistance $\tau_{bed,exp}+\tau_{veg,exp}$), (b) Bed resistance ratio, (c) Vegetation resistance ratio, (d) Flow discharge.

CONCLUSIONS

Previous studies have focused on vegetation resistance with the impact of vegetation being ignored or poorly estimated. In order to quantify bed resistance and vegetation resistance, a new analytical model has been proposed in this study based on the momentum conservation law. Considering the effect of vegetation on the flow structure, two correction coefficients are introduced to modify the logarithmic and uniform velocity distributions. The model is verified against five sets of laboratory experiments. The following conclusions can be drawn from the results:

1) With the velocity distribution modification, the proposed model is capable of reasonably resolving resistance to open channel flow with emergent vegetation. Comparatively speaking, the version of the model that assumes a modified logarithmic velocity profile performs better than that based on a modified uniform velocity distribution.

2) The ratio of bed resistance to total flow resistance ranges between 5% and 40%, and generally decreases with the increase in vegetation density and water depth. For relatively shallow flow with sparse vegetation, the bed resistance therefore becomes more important and cannot be ignored, especially when sediment transport is involved.

3) With the modified coefficient used to account for the effect of vegetation arrangement, the model performance has further improved. It has also been demonstrated that the modified coefficient for vegetation arrangement does not vary proportionally with vegetation density but increases with the number of vegetation plants per unit bed area.

The present analytical model explicitly quantifies the bed resistance and vegetation resistance of emergent rigid vegetated flows without bed forms and fully considers the effects of vegetation density and vegetation arrangement on vegetation resistance. In future investigations, the present model could be incorporated into the shallow water equations to replace Manning's coefficient that is usually estimated empirically. In this way, a modified hydrodynamic model of rigid vegetated flow may be developed. The model could then accurately simulate the effect of vegetation on flood propagation, which is no longer limited by the preconditions of the roughness empirical equation. Meanwhile, the solution of the friction velocity facilitates a basis for the numerical modeling of flow and sediment transport in vegetated channels.

CRediT authorship contribution statement. Jiangyu Wang: Methodology, Data curation, Software, Visualization, Writing – original draft. Jinxin Liu: Investigation, Methodology, Writing – original draft. Yining Sun: Visualization, Writing - review & editing; Ji Li: Writing - review & editing; Zhixian Cao: Conceptualization, Methodology, Investigation, Supervision, Writing - Review & editing.

Declaration of Competing Interest. The authors declare that they have no known competing financial interests or personal relationships that could have appeared to influence the work reported in this paper.

Data availability. Data will be made available on request.

Acknowledgments. This work has been funded by the National Natural Science Foundation of China under Grant No. 52239007.

REFERENCES

Aberle, J., Järvelä, J., 2013. Flow resistance of emergent rigid and flexible floodplain vegetation. J. Hydraul. Res., 51, 33–45. https://doi.org/10.1080/00221686.2012.754795

Afzalimehr, H., Dey, S., 2009. Influence of bank vegetation and gravel bed on velocity and Reynolds stress distributions. Int. J. Sediment Res., 24, 236–246. https://doi.org/10.1016/S1001-6279(09)60030-5

Alekseevskiy, N.I., Berkovich, K.M., Chalov, R.S., 2008. Erosion, sediment transportation and accumulation in rivers. Int. J. Sediment Res., 23, 93–105. https://doi.org/10.1016/S1001-6279(08)60009-8

Armanini, A., Righetti, M., Grisenti, P., 2005. Direct measurement of vegetation resistance in prototype scale. J. Hydraul. Res., 43, 481–487. https://doi.org/10.1080/00221680509500146

Baptist, M.J., Babovic, V., Rodríguez Uthurburu, J., Keijzer, M., Uittenbogaard, R.E., Mynett, A., Verwey, A., 2007. On inducing equations for vegetation resistance. J. Hydraul. Res., 45, 435–450. https://doi.org/10.1080/00221686.2007.9521778

Ben Meftah, M., Mossa, M., 2016. A modified log-law of flow velocity distribution in partly obstructed open channels. Environ. Fluid Mech., 16, 453–479. https://doi.org/10.1007/s10652-015-9439-7

Bennett, S.J., Pirim, T., Barkdoll, B.D., 2002. Using simulated emergent vegetation to alter stream flow direction within a straight experimental channel. Geomorphology, 44, 115–126. https://doi.org/10.1016/S0169-555X(01)00148-9

Chapman, J.A., Wilson, B.N., Gulliver, J.S., 2015. Drag force parameters of rigid and flexible vegetal elements: drag resistance from flexible vegetal elements. Water Resour. Res., 51, 3292–3302. https://doi.org/10.1002/2014WR015436

Cheng, N.S., 2011. Representative roughness height of submerged vegetation: representative roughness height of submerged vegetation. Water Resour. Res., 47. https://doi.org/10.1029/2011WR010590

Cheng, N.S., Nguyen, H.T., 2011. Hydraulic radius for evaluating resistance induced by simulated emergent vegetation in open-channel flows. J. Hydraul. Eng., 137, 995–1004. https://doi.org/10.1061/(ASCE)HY.1943-7900.0000377

D'Ippolito, A., Lauria, A., Alfonsi, G., Calomino, F., 2019. Investigation of flow resistance exerted by rigid emergent vegetation in open channel. Acta Geophys., 67, 971–986. https://doi.org/10.1007/s11600-019-00280-8

Fathi-Maghadam, M., Kouwen, N., 1997. Nonrigid, nonsubmerged, vegetative roughness on floodplains. J. Hydraul. Eng., 123, 51–57. https://doi.org/10.1061/(ASCE)0733-9429(1997)123:1(51)

Gu, F.F., Ni, H.G., Qi, D.M., 2007. Roughness coefficient for unsubmerged and submerged reed. J. Hydrodyn., 19, 421–428. https://doi.org/10.1016/S1001-6058(07)60135-8

Gurnell, A.M., Bertoldi, W., Corenblit, D., 2012. Changing river channels: The roles of hydrological processes, plants and pioneer fluvial landforms in humid temperate, mixed load, gravel bed rivers. Earth Sci. Rev., 111, 129–141. https://doi.org/10.1016/j.earscirev.2011.11.005

Huai, W.X., Chen, Z.B., Han, J., Zhang, L.X., Zeng, Y.H., 2009a. Mathematical model for the flow with submerged and emerged rigid vegetation. J. Hydrodyn., 21, 722–729. https://doi.org/10.1016/S1001-6058(08)60205-X

Huai, W.X., Shi, H.R., Song, S.W., Ni, S.Q., 2018. A simplified method for estimating the longitudinal dispersion coefficient in ecological channels with vegetation. Ecol. Indic., 92, 91–98. https://doi.org/10.1016/j.ecolind.2017.05.015

Huai, W.X., Xue, W.Y., Qian, Z.D., 2015. Large-eddy

simulation of turbulent rectangular open-channel flow with an emergent rigid vegetation patch. Adv. Water Resour., 80, 30–42. https://doi.org/10.1016/j.advwatres.2015.03.006

Huai, W.X., Zeng, Y.H., Xu, Z.G., Yang, Z.H., 2009b. Three-layer model for vertical velocity distribution in open channel flow with submerged rigid vegetation. Adv. Water Resour., 32, 487–492. https://doi.org/10.1016/j.advwatres.2008.11.014

Hui, E.Q., Hu, X.E., Jiang, C., Ma, F.K., Zhu, Z.D., 2010. A study of drag coefficient related with vegetation based on the flume experiment. J. Hydrodyn., 22, 329–337. https://doi.org/10.1016/S1001-6058(09)60062-7

James, C.S., 2021. Flow resistance in channels with large emergent roughness elements. J. S. Afr. Inst. Civ. Eng., 63, 1–9. https://doi.org/10.17159/2309-8775/2021/v63n4a1

James, C.S., Birkhead, A.L., Jordanova, A.A., O'Sullivan, J.J., 2004. Flow resistance of emergent vegetation. J. Hydraul. Res., 42, 390–398. https://doi.org/10.1080/00221686.2004.9728404

Järvelä, J., 2002. Flow resistance of flexible and stiff vegetation: a flume study with natural plants. J. Hydrol., 269, 44–54. https://doi.org/10.1016/S0022-1694(02)00193-2

Jordanova, A., James, C., 2003. Experimental study of bed load transport through emergent vegetation. J. Hydraul. Eng.-ASCE, 129, 474–478. https://doi.org/10.1061/(ASCE)0733-9429(2003)129:6(474)

Jordanova, A.A., James, C.S., Birkhead, A.L., 2006. Practical estimation of flow resistance through emergent vegetation. Proc. Inst. Civil. Eng.-Water Manag., 159, 173–181.

Klopstra, D., Barneveld, H.J., Noortwijk, J.M.V., Velzen, E.H.V., 1997. Analytical model for hydraulic roughness of submerged vegetation. In: Proc. 27th Congress of the International Association of Hydraulic Research, ASCE, San Francisco, USA, pp. 775–780.

Kothyari, U.C., Hayashi, K., Hashimoto, H., 2009. Drag coefficient of unsubmerged rigid vegetation stems in open channel flows. J. Hydraul. Res., 47, 691–699. https://doi.org/10.3826/jhr.2009.3283

Kouwen, N., Fathi-Moghadam, M., 2000. Friction factors for coniferous trees along rivers. J. Hydraul. Eng., 126, 732–740. https://doi.org/10.1061/(ASCE)0733-9429(2000)126:10(732)

Kumar, P., Sharma, A., 2022. Experimental investigation of 3D flow properties around emergent rigid vegetation. Ecohydrol., 15. https://doi.org/10.1002/eco.2474

Li, S.L., Shi, H.R., Xiong, Z.W., Huai, W.X., Cheng, N.S., 2015. New formulation for the effective relative roughness height of open channel flows with submerged vegetation. Adv. Water Resour., 86, 46–57. https://doi.org/10.1016/j.advwatres.2015.09.018

Li, Y.P., Anim, D.O., Wang, Y., Tang, C.Y., Du, W., Yu, Z.B., Acharya, K., 2014. An open-channel flume study of flow characteristics through a combined layer of submerged and emerged flexible vegetation: flow characteristics through submerged and emerged flexible vegetation. Ecohydrol., 7, 633–647. https://doi.org/10.1002/eco.1384

Liu, D., Diplas, P., Fairbanks, J.D., Hodges, C.C., 2008. An experimental study of flow through rigid vegetation. J. Geophys. Res., 113, F04015. https://doi.org/10.1029/2008JF001042

Liu, M.Y., Huai, W.X., Yang, Z.H., Zeng, Y.H., 2020. A genetic programming-based model for drag coefficient of emergent vegetation in open channel flows. Adv. Water Resour., 140, 103582. https://doi.org/10.1016/j.advwatres.2020.103582

López, F., García, M.H., 2001. Mean flow and turbulence structure of open-channel flow through non-emergent vegetation. J. Hydraul., Eng. 127, 392–402. https://doi.org/10.1061/(ASCE)0733-9429(2001)127:5(392)

Michioku, K., Kometani, S., Uotani, T., Kanda, K., Irie, Y., Yanagida, K., 2014. Analysis of equivalent Manning's roughness coefficient for trees vegetated on floodplain. In: Proc. 7th Int. Conf. on Fluvial Hydraulics (River Flow), pp. 563–570.

Millar, R.G., 2000. Influence of bank vegetation on alluvial channel patterns. Water Resour. Res., 36, 1109–1118. https://doi.org/10.1029/1999WR900346

Nezu, I., Sanjou, M., 2008. Turburence structure and coherent motion in vegetated canopy open-channel flows. J. Hydro-Environ. Res., 2, 62–90. https://doi.org/10.1016/j.jher.2008.05.003

Nikora, N., Nikora, V., O'Donoghue, T., 2013. Velocity profiles in vegetated open-channel flows: combined effects of multiple mechanisms. J. Hydraul. Eng., 139, 1021–1032. https://doi.org/10.1061/(ASCE)HY.1943-7900.0000779

Noarayanan, L., Murali, K., Sundar, V., 2012. Manning's 'n' coefficient for flexible emergent vegetation in tandem configuration. J. Hydro-Environ. Res., 6, 51–62. https://doi.org/10.1016/j.jher.2011.05.002

Osterkamp, W.R., Hupp, C.R., 2010. Fluvial processes and vegetation – Glimpses of the past, the present, and perhaps the future. Geomorphology, 116, 274–285. https://doi.org/10.1016/j.geomorph.2009.11.018

Poggi, D., Krug, C., Katul, G.G., 2009. Hydraulic resistance of submerged rigid vegetation derived from first-order closure models: hydraulic resistance of submerged rigid vegetation. Water Resour. Res., 45. https://doi.org/10.1029/2008WR007373

Rowiński, P.M., Kubrak, J., 2002. A mixing-length model for predicting vertical velocity distribution in flows through emergent vegetation. Hydrol. Sci., J. 47, 893–904. https://doi.org/10.1080/02626660209492998

Schlichting, H., Gersten, K., 1979. Boundary-Layer Theory. McGraw-Hill, New York.

Stephan, U., Gutknecht, D., 2002. Hydraulic resistance of submerged flexible vegetation. J. Hydrol., 269, 27–43. https://doi.org/10.1016/S0022-1694(02)00192-0

Stoesser, T., Kim, S.J., Diplas, P., 2010. Turbulent flow through idealized emergent vegetation. J. Hydraul. Eng. 136, 1003–1017. https://doi.org/10.1061/(ASCE)HY.1943-7900.0000153

Stone, B.M., Shen, H.T., 2002. Hydraulic resistance of flow in channels with cylindrical roughness. J. Hydraul. Eng., 128, 500–506. https://doi.org/10.1061/(ASCE)0733-9429(2002)128:5(500)

Tanino, Y., Nepf, H.M., 2008. Laboratory investigation of mean drag in a random array of rigid, emergent cylinders. J. Hydraul. Eng., 134, 34–41. https://doi.org/10.1061/(ASCE)0733-9429(2008)134:1(34)

Tang, H.W., Yan, J., Xiao, Y., Lu, S.Q.,2007. Manning's roughness coefficient of vegetated channels. J. Hydraul. Eng., 38, 11, 1347–1353. (In Chinese.)

Tinoco, R.O., Cowen, E.A., 2013. The direct and indirect measurement of boundary stress and drag on individual and complex arrays of elements. Exp. Fluids, 54, 1509. https://doi.org/10.1007/s00348-013-1509-3

Vargas-Luna, A., Crosato, A., Calvani, G., Uijttewaal, W.S.J., 2016. Representing plants as rigid cylinders in experiments and models. Adv. Water Resour., 93, 205–222. https://doi.org/10.1016/j.advwatres.2015.10.004

Wang, H., Tang, H.W., Yuan, S.Y., Lv, S.Q., Zhao, X.Y., 2014. An experimental study of the incipient bed shear stress partition in mobile bed channels filled with emergent rigid vegetation. Sci. China-Technol. Sci., 57, 1165–1174. https://doi.org/10.1007/s11431-014-5549-6

Wang, J.S., Liu, X.G., Min, F.Y., Dai, J., Jiang, X., 2022. Turbulence structure and longitudinal velocity distribution of open channel flows with reedy emergent vegetation. Ecohydrol., 15. https://doi.org/10.1002/eco.2352

Wohl, E., Angermeier, P.L., Bledsoe, B., Kondolf, G.M.,

MacDonnell, L., Merritt, D.M., Palmer, M.A., Poff, N.L., Tarboton, D., 2005. River restoration: opinion. Water Resour. Res., 41. https://doi.org/10.1029/2005WR003985

Wu, F.C., Shen, H.W., Chou, Y.J., 1999. Variation of roughness coefficients for unsubmerged and submerged vegetation. J. Hydraul. Eng., 125, 934–942. https://doi.org/10.1061/(ASCE)0733-9429(1999)125:9(934)

Wu, F.S., 2008. Characteristics of flow resistance in open channels with non-submerged rigid vegetation. J. Hydrodyn., 20, 239–245. https://doi.org/10.1016/S1001-6058(08)60052-9

Wu, W.M., He, Z.G., 2009. Effects of vegetation on flow conveyance and sediment transport capacity. Int. J. Sediment Res., 24, 247–259. https://doi.org/10.1016/S1001-6279(10)60001-7

Yang, Z.H., Li, D., Huai, W.X., Liu, J.H., 2019. A new method to estimate flow conveyance in a compound channel with vegetated floodplains based on energy balance. J. Hydrol., 575, 921–929. https://doi.org/10.1016/j.jhydrol.2019.05.078

Zhao, K.F., Cheng, N.S., Huang, Z.H., 2014a. Experimental study of free-surface fluctuations in open-channel flow in the presence of periodic cylinder arrays. J. Hydraul. Res., 52, 465–475. https://doi.org/10.1080/00221686.2014.880858

Zhao, K.F., Cheng, N.S., Wang, X.K., Tan, S.K., 2014b. Measurements of fluctuation in drag acting on rigid cylinder array in open channel flow. J. Hydraul. Eng., 140, 48–55. https://doi.org/10.1061/(ASCE)HY.1943-7900.0000811

Zhao, M.D., Fan, Z.L., 2019. Emergent vegetation flow with varying vertical porosity. J. Hydrodyn., 31, 1043–1051. https://doi.org/10.1007/s42241-018-0083-9

Zhang, Y.G., Wang, P., Cheng, J.H., Wang, W.J., Zeng, L., Wang, B., 2020. Drag coefficient of emergent flexible vegetation in steady nonuniform flow. Water Resour. Res., 56. https://doi.org/10.1029/2020WR027613

Received 13 November 2023
Accepted 12 March 2024

Appendix I: Summary of flume experimental data

Investigator	Case	B (m)	D (m)	ϕ (%)	Q (m^3/s)	h (m)	S (–)
Tang et al. (2007)	A-1	0.42	/	/	0.00756	0.06	0.00055
	A-2	0.42	/	/	0.01134	0.09	0.00041
	A-3	0.42	/	/	0.01512	0.12	0.00030
	A-4	0.42	/	/	0.01890	0.15	0.00025
	A-5	0.42	/	/	0.02168	0.18	0.00020
	B-1	0.42	0.006	2.83	0.00680	0.09	0.01000
	B-2	0.42	0.006	2.83	0.00917	0.12	0.01100
	B-3	0.42	0.006	2.83	0.01134	0.15	0.01100
	B-4	0.42	0.006	2.83	0.01370	0.18	0.01200
	C-1	0.42	0.006	1.13	0.01110	0.09	0.01100
	C-2	0.42	0.006	1.13	0.01512	0.12	0.01100
	C-3	0.42	0.006	1.13	0.01820	0.15	0.01100
	C-4	0.42	0.006	1.13	0.02192	0.18	0.01100
James (2021)	D-1	2	/	/	0.00944	0.02	0.00075
	D-2	2	/	/	0.02064	0.04	0.00075
	D-3	2	/	/	0.03136	0.05	0.00075
	D-4	2	/	/	0.03835	0.05	0.00075
	D-5	2	/	/	0.05339	0.07	0.00075
	E-1	2	0.1100	1.51	0.01674	0.05	0.00050
	E-2	2	0.1100	1.51	0.02275	0.06	0.00050
	E-3	2	0.1100	1.51	0.03168	0.08	0.00050
	E-4	2	0.1100	1.51	0.03846	0.10	0.00050
	E-5	2	0.1100	1.51	0.04360	0.11	0.00050
	F-1	2	0.1100	3.03	0.01178	0.05	0.00050
	F-2	2	0.1100	3.03	0.02076	0.08	0.00050
	F-3	2	0.1100	3.03	0.02812	0.11	0.00050
	F-4	2	0.1100	3.03	0.03707	0.14	0.00050
	F-5	2	0.1100	3.03	0.04380	0.17	0.00050
D'Ippolito et al. (2019)	G-1	0.382	0.0080	0.78	0.00577	0.07	0.00480
	G-2	0.382	0.0080	0.78	0.00860	0.09	0.00480
	G-3	0.382	0.0080	0.78	0.01165	0.11	0.00480
	G-4	0.382	0.0080	0.78	0.01462	0.13	0.00480
	H-1	0.382	0.0100	0.97	0.00307	0.04	0.00480
	H-2	0.382	0.0100	0.97	0.00536	0.07	0.00480
	H-3	0.382	0.0100	0.97	0.00795	0.10	0.00480
	I-1	0.382	0.0080	2.79	0.00583	0.07	0.01350
	I-2	0.382	0.0080	2.79	0.00577	0.08	0.01350
	I-3	0.382	0.0080	2.79	0.00855	0.10	0.01350
	I-4	0.382	0.0080	2.79	0.01161	0.12	0.01350
Cheng and Nguyen (2011)	J-1	0.3	0.0032	0.43	0.00071	0.02	0.00186
	J-2	0.3	0.0032	0.43	0.00114	0.03	0.00186
	J-3	0.3	0.0032	0.43	0.00158	0.04	0.00186
	J-4	0.3	0.0032	0.43	0.00200	0.05	0.00186
	J-5	0.3	0.0032	0.43	0.00247	0.06	0.00186
	J-6	0.3	0.0032	0.43	0.00284	0.07	0.00186
	J-7	0.3	0.0032	0.43	0.00374	0.09	0.00186
	J-8	0.3	0.0032	0.43	0.00412	0.10	0.00186
	K-1	0.3	0.0066	1.92	0.00053	0.03	0.00122
	K-2	0.3	0.0066	1.92	0.00066	0.04	0.00122
	K-3	0.3	0.0066	1.92	0.00083	0.05	0.00122
	K-4	0.3	0.0066	1.92	0.00108	0.06	0.00122
	K-5	0.3	0.0066	1.92	0.00128	0.07	0.00122

	K-6	0.3	0.0066	1.92	0.00141	0.08	0.00122
	K-7	0.3	0.0066	1.92	0.00159	0.09	0.00122
	K-8	0.3	0.0066	1.92	0.00184	0.10	0.00122
	K-9	0.3	0.0066	1.92	0.00049	0.02	0.00196
	K-10	0.3	0.0066	1.92	0.00068	0.03	0.00196
	K-11	0.3	0.0066	1.92	0.00096	0.04	0.00196
	K-12	0.3	0.0066	1.92	0.00126	0.05	0.00196
	K-13	0.3	0.0066	1.92	0.00149	0.06	0.00196
	K-14	0.3	0.0066	1.92	0.00181	0.07	0.00196
	K-15	0.3	0.0066	1.92	0.00207	0.08	0.00196
	K-16	0.3	0.0066	1.92	0.00222	0.09	0.00196
	K-17	0.3	0.0066	1.92	0.00251	0.10	0.00196
	K-18	0.3	0.0066	1.92	0.00064	0.02	0.00410
	K-19	0.3	0.0066	1.92	0.00097	0.03	0.00410
	K-20	0.3	0.0066	1.92	0.00141	0.04	0.00410
	K-21	0.3	0.0066	1.92	0.00174	0.05	0.00410
	K-22	0.3	0.0066	1.92	0.00213	0.06	0.00410
	K-23	0.3	0.0066	1.92	0.00254	0.07	0.00410
	K-24	0.3	0.0066	1.92	0.00295	0.08	0.00410
	K-25	0.3	0.0066	1.92	0.00329	0.09	0.00410
	K-26	0.3	0.0066	1.92	0.00380	0.10	0.00410
	K-27	0.3	0.0066	1.92	0.00106	0.02	0.00811
	K-28	0.3	0.0066	1.92	0.00140	0.03	0.00811
	K-29	0.3	0.0066	1.92	0.00197	0.04	0.00811
	K-30	0.3	0.0066	1.92	0.00258	0.05	0.00811
	K-31	0.3	0.0066	1.92	0.00319	0.06	0.00811
	K-32	0.3	0.0066	1.92	0.00375	0.07	0.00811
	K-33	0.3	0.0066	1.92	0.00429	0.08	0.00811
	K-34	0.3	0.0066	1.92	0.00484	0.09	0.00811
	K-35	0.3	0.0066	1.92	0.00545	0.10	0.00811
	L-1	0.3	0.0083	2.98	0.00061	0.04	0.00100
	L-2	0.3	0.0083	2.98	0.00097	0.06	0.00100
	L-3	0.3	0.0083	2.98	0.00135	0.08	0.00100
	L-4	0.3	0.0083	2.98	0.00131	0.09	0.00100
	L-5	0.3	0.0083	2.98	0.00143	0.10	0.00100
	L-6	0.3	0.0083	2.98	0.00062	0.03	0.00200
	L-7	0.3	0.0083	2.98	0.00075	0.04	0.00200
	L-8	0.3	0.0083	2.98	0.00122	0.06	0.00200
	L-9	0.3	0.0083	2.98	0.00174	0.08	0.00200
	L-10	0.3	0.0083	2.98	0.00189	0.09	0.00200
	L-11	0.3	0.0083	2.98	0.00221	0.10	0.00200
	L-12	0.3	0.0083	2.98	0.00083	0.03	0.00400
	L-13	0.3	0.0083	2.98	0.00107	0.04	0.00400
	L-14	0.3	0.0083	2.98	0.00171	0.06	0.00400
	L-15	0.3	0.0083	2.98	0.00283	0.08	0.00400
	L-16	0.3	0.0083	2.98	0.00274	0.09	0.00400
	L-17	0.3	0.0083	2.98	0.00319	0.10	0.00400
Zhao et al. (2014a)	M-1	0.3	0.0083	1.3	0.00581	0.072	0.01020
	M-2	0.3	0.0083	1.3	0.00658	0.091	0.00830
	M-3	0.3	0.0083	1.3	0.00518	0.081	0.00630
	M-4	0.3	0.0083	1.3	0.00482	0.087	0.00500
	M-5	0.3	0.0083	1.3	0.00430	0.078	0.00500
	M-6	0.3	0.0083	1.3	0.00422	0.071	0.00440